Histol Histopathol (2017) 32: 571-584

http://www.hh.um.es

Histology and Histopathology

From Cell Biology to Tissue Engineering

Morphometric characterization of the human portal and hepatic venous trees: A quantitative support to the liver micro-anatomic models free of subunits

Sergio Almenar-Medina[1], Brenda Palomar-De Lucas[1], Ester Guerrero-Albors[1] and Amparo Ruiz-Sauri[2]

[1]Fundación Instituto Valenciano de Oncología (FIVO) and

[2]Departament of Pathology, Faculty of Medicine and Odontology, University of Valencia, Valencia, Spain

Summary. Conventional models of liver microanatomy assume the presence of subunits. Nevertheless, some researchers propose that the liver is a continuous structure, free of these subunits, but with a characteristic vascular pattern. The present study describes a morphometric analysis of portal and hepatic veins in 50 human autopsy non-pathological liver samples.

The main objective was to measure three proportions: 1. portal tracts / hepatic veins, 2. distributing portal veins / distributing hepatic veins and 3. terminal portal veins / terminal hepatic veins. These ratios were compared with the traditional microcirculatory liver models.

Our material comprised 3,665 portal veins and 3,761 hepatic veins. The minimum diameter of half of the venous vessels of both types belongs to the interval (25 μm , 60 μm), given that 1881 portal veins (49.434%) and 1924 hepatic veins (50.565%) fall within this interval. We have statistically shown with the χ^2 test (α=0.990) that the portal and hepatic veins belonging to the interval (25 μm, 400 μm) (distributing veins) had an identical proportion.

If the portal and hepatic veins are arranged according to the principle of interdigitation of Takashasi (1970), there should be an almost identical number of both types of veins. Our results contradict the presumably numeric preponderance of distributing portal veins with regard to the distributing hepatic veins that is inherent in the models of Kiernan, Matsumoto and Rappaport.

Key words: Liver microvasculature, Liver morphometry, Liver subunits.

Offprint requests to: Sergio Almenar-Medina, Fundación Instituto Valenciano de Oncología (FIVO), Valencia, Spain. e-mail: sergioalmenarmedina@gmail.com

DOI: 10.14670/HH-11-823

Introduction

From Kiernan (1833) to the present day, numerous microanatomists have searched for a hepatic subunit whose spatial repetition originates the whole organ. The morphology of these hypothetical subunits is controversial, thus various models have been proposed.

The classic lobule described in the adult pig by Kiernan (1833) is a parenchymatous hexagonal prism enveloped by connective septa. At their edges there are interlobular portal tracts (ILPTs) containing an interlobular portal vein (ILPV), one or more arterioles and one or more bile ducts. In its central axis lies a centrilobular hepatic vein (CLHV) connected with the ILPV by means of sinusoids (Fig. 1A). However, in man, rat, and even in the suckling pig, these structures

Abbreviations. ADV(s): Axial Distributing Vein(s). CHV(s): Conducting Hepatic Vein(s). CLHV(s): CentriLobular Hepatic Vein(s). CPV(s): Conducting Portal Vein(s). DPV(s): Distributing Portal Vein(s). HV(s): Hepatic Vein(s). ILPT(s): InterLobular Portal Tract(s). ILPV(s): InterLobular Portal Vein(s). MDV(s): Marginal Distributing Vein(s). PT(s): Portal Tract(s). PTPT(s): PreTerminal Portal Tract(s). PTPV(s): PreTerminal Portal Vein(s). PV(s): Portal Vein(s). THV(s): Terminal Hepatic Vein(s). TPT(s): Terminal Portal Tract(s). TPV(s): Terminal Portal Vein(s).

were not observed (Elias, 1963). The Kiernan lobule maintains a certain morphological relation to the secondary lobule of Matsumoto and Kawakami (1982) (Fig. 1B).

Considering the liver as an exocrine gland, Mall (1906) introduced the portal lobule subunit as a parenchymal triangular prism with a portal tract (PT) in its center and three hepatic veins (HVs) on the edges (Fig. 1C).

Rappaport et al. (1954) and Rappaport (1973) proposed that the simple liver acinus (with a "rugby ball" shape) is the fundamental subunit of the liver. It consists of three concentric zones of parenchyma depending on the degree of oxygenation. Its anatomical axis is a terminal portal tract (TPT) containing a terminal portal vein (TPV), arteriole(s), and terminal bile duct(s). The complex acinus consists of three simple acini that spring from a preterminal portal tract (PTPT) (the classic ILPT) (Fig. 1D).

Opposing the models based on the existence of subunits, Elias (1949a,b) attacked the idea of modularity finding that the hepatic parenchyma consists of a continuous muralium of one hepatocyte of thickness, which extends along the entire gland. He said, "lobules are imaginary areas which can be created arbitrarily around portal canals or around hepatic vein roots" (Elias, 1963).

Takahashi (1970), with a similar point of view, considers that "the histological structure of the human liver seems to be quite simple: a continuous mass of parenchymal tissue is penetrated by portal tracts and hepatic veins". He also states that the liver architecture can be described on the principle of vascular interdigitation. The "interdigitation is a condition in which the terminal afferent and efferent vessels are arranged alternately at some distances from each other". (Fig. 2).

More recently, the "hepatic enzymic zonation" studies (Lamers et al., 1989) and tridimensional reconstructions (Ishikawa et al., 2000) also question the modularity of the liver parenchyma. Lamers et al. (1989) found that the parenchyma that express carbamoylphosphate synthetase located around the portal spaces delimits a continuous three-dimensional network enveloping the parenchyma that exhibits glutamine synthetase distributed around the branches of the hepatic veins. An important consequence is the observation that, in two dimensions, the latter territory exhibits a round contour. Moreover, Rømert et al. (1993), evaluating colloidal gold uptake, found microcirculatory free of metal zones concentric with the terminal hepatic veins (THVs). This round morphology and concentric distribution around the THVs contradicts the idea of Rappaport (Fig. 1D).

Ishikawa et al. (2000) found that the round to oval parenchymatous islands of fatty livers from diabetic

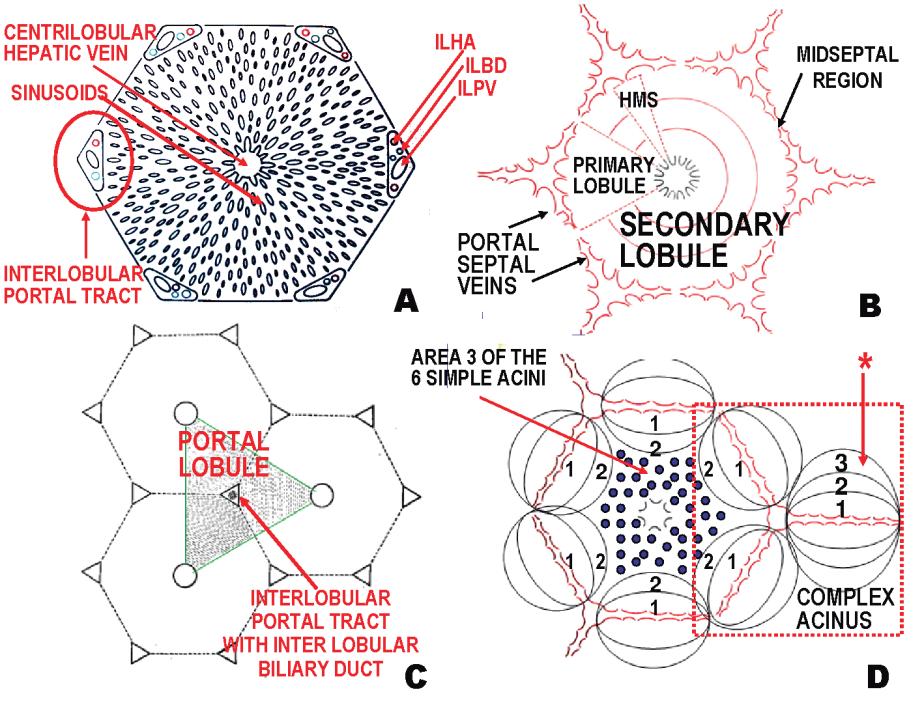

Fig. 1. A. Two-dimensional section of the Kiernan lobule. ILBD: Inter-lobular bile duct. ILHA: Inter-lobular hepatic artery. ILPV: Inter-lobular portal vein. CLHV: Centrilobular hepatic vein. **B.** The secondary lobule of Matsumoto and Kawakami (1982) which consists of six primary lobules of conic morphology. Its vertices are in contact with the terminal hepatic vein (classic centrilobular vein). Its convex side contains a portal tract and two septal portal veins. The vascular septa of the Matsumoto lobule replace the connective septa of the classic Kiernan lobule. Vascular septa ensure a perfusion pressure equally distributed among all points of a circle centered on the terminal hepatic vein. McCuskey (1993, 1994 and 2008) have introduced a further refinement. The Hepatic Microcirculatory Subunit (HMS) corresponds to a conical liver parenchymal territory supplied by an inlet venule. **C**. Two-dimensional section of the portal lobule with three terminal hepatic veins (THV) at their edges and a portal tract in the center with a interlobular bile duct. **D.** Rappaport model. Seven simple acini (three forming part of a complex acinus) are represented. The three areas are drawn in only one acinus (asterisk). The area resulting from the confluence of area 3 of the 6 simple acini would have a star-like form with its rays in contact with the portal tracts (area with round spots that in theory corresponds to porto-centrilobular bridges after hepatocyte necrosis). However, Nakamura and Takahashi (1998), studying the geometry of acute and chronic zonal necrosis, establish that these necrotic areas never reach the PTs. Furthermore, the Rappaport model does not satisfactorily explain the genesis of incomplete septal cirrhosis (Wanless et al. 2000).

shrews have a similar morphology and distribution to those observed in mouse liver necrosis produced by CCl_4. The systematic tridimensional reconstruction of the alive and necrotic zones allows the assumption that the liver parenchyma consists of two continuous domains (pericentral and periportal). This structural continuity also contradicts the classic subunit conception.

Considering that the vascular tree has a decisive influence during liver organogenesis (Kuo et al., 1991; Matsumoto et al., 2001; Matsumoto et al., 2008; Korzh et al., 2008; Cast et al., 2015) it is permissible to draw conclusions about liver structure from the study of the distribution of its vessels.

Materials and methods

The present observational and retrospective study was approved by the Ethics Committee of Clinical Research from *FIVO* (Fundación Instituto Valenciano de Oncología), April 7, 2014

Study population and liver tissue samples

Formalin-fixed, paraffin-embedded liver tissues were retrieved from 50 autopsies during the period 1990-2013. At the time of death, these patients had no clinical or analytical alterations suggestive of liver disease. Furthermore, an histological confirmation (with conventional H&E stain) in order to exclude any hepatic parenchymal structural alteration was performed.

Staining of the samples

With each of these paraffin blocks two sections 6 μm thick were stained with HE and reticulin (Impregnazione argentica per reticolo®, BIOPTICA). The latter technique shows the layout of the fibrillar frame of sinusoids and veins.

Anatomical criteria

The portal veins (PVs) with a diameter higher than 400 μm were classified as Conducting Portal Veins (CPVs) (Elias, 1963; Jones and Spring-Mills, 1982). Therefore, the interlobar, segmental, and subsegmental PVs are CPVs. Portal venous branches with a diameter less than 400 μm were considered as distributing portal veins (DPVs). Therefore, the ILPVs (or PTPVs), TPVs and inlet veins fall in the category of DPVs. According to the Elias (1963) criteria, the DPVs are of two types: marginal distributing veins (MDVs) and axial distributing veins (ADVs). The MDVs run through the same portal tract as the CPV of origin. The ADVs have a diameter less than 280 μm and these vessels are not accompanied by any other portal vessel (they are the only distributing vein within a portal tract). Those DPVs with a diameter between 400 μm and 280 μm have mixed properties: they can give rise to another DPV (running through the same portal tract) (Fig. 3A) as well as inlet venules.

According to Gibson (1959) conducting hepatic veins (CHVs) have a diameter in the interval [1cm, 400

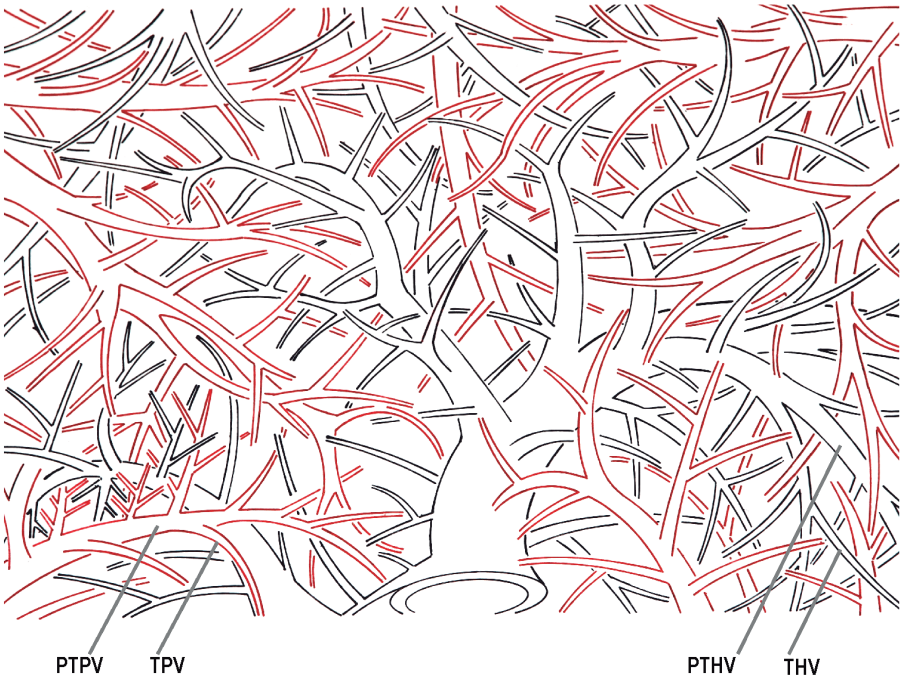

Fig. 2. Takahashi model. The portal tree is marked in red and the hepatic vein tree in black. TPV: Terminal Portal Veins. THV: Terminal Hepatic Vein. PTPV: Pre-Terminal Portal Vein. PTHV: Pre-Terminal Hepatic Vein. This drawing is a free-reproduction of the lamina present in the work of Takahashi (1970), adding more terminal vessels of both circulations. The interdigitation of these vessels and their equidistant disposition are the major characteristics of this model.

μm), the sublobular or intercalated veins in the interval [400 μm, 100 μm) and the terminal hepatic veins (THVs) within the interval [100 μm, 25 μm). However, Porto et al. (1989a) consider as THVs those with an internal diameter ≤150 μm. However, at histological level, THVs show a narrow periendothelial connective rim with a lumen in continuity with multiple sinusoidal spaces (Crawford et al. 1998) (Fig. 3C,D).

Due to the difference in numerical criteria among diverse authors, the venous vessels of both systems will be compared considering diametric intervals.

We only studied, counted and measured as PTs those structures with connective tissue having one or more portal veins, one or more arterioles, and one or more bile ducts (each with a continuous connective tissue envelope) (Fig. 3A,B).

We did not take into account solitary profiles or dyads (Crawford et al., 1998), only considering as HVs these vascular structures located outside the portal tracts.

Confusing a HV with a hypothetical PV solitary profile is unlikely, since an increased amount of connective tissue between the vein and the limiting plate indicates a PV solitary profile.

The so-called "isolated artery" (Ekataksin, 2000) is a small-caliber vessel surrounded by a clear smooth muscle layer identifiable with conventional histological methods. This vessel could never be confused with a hepatic sublobular vein (striated), since these do not

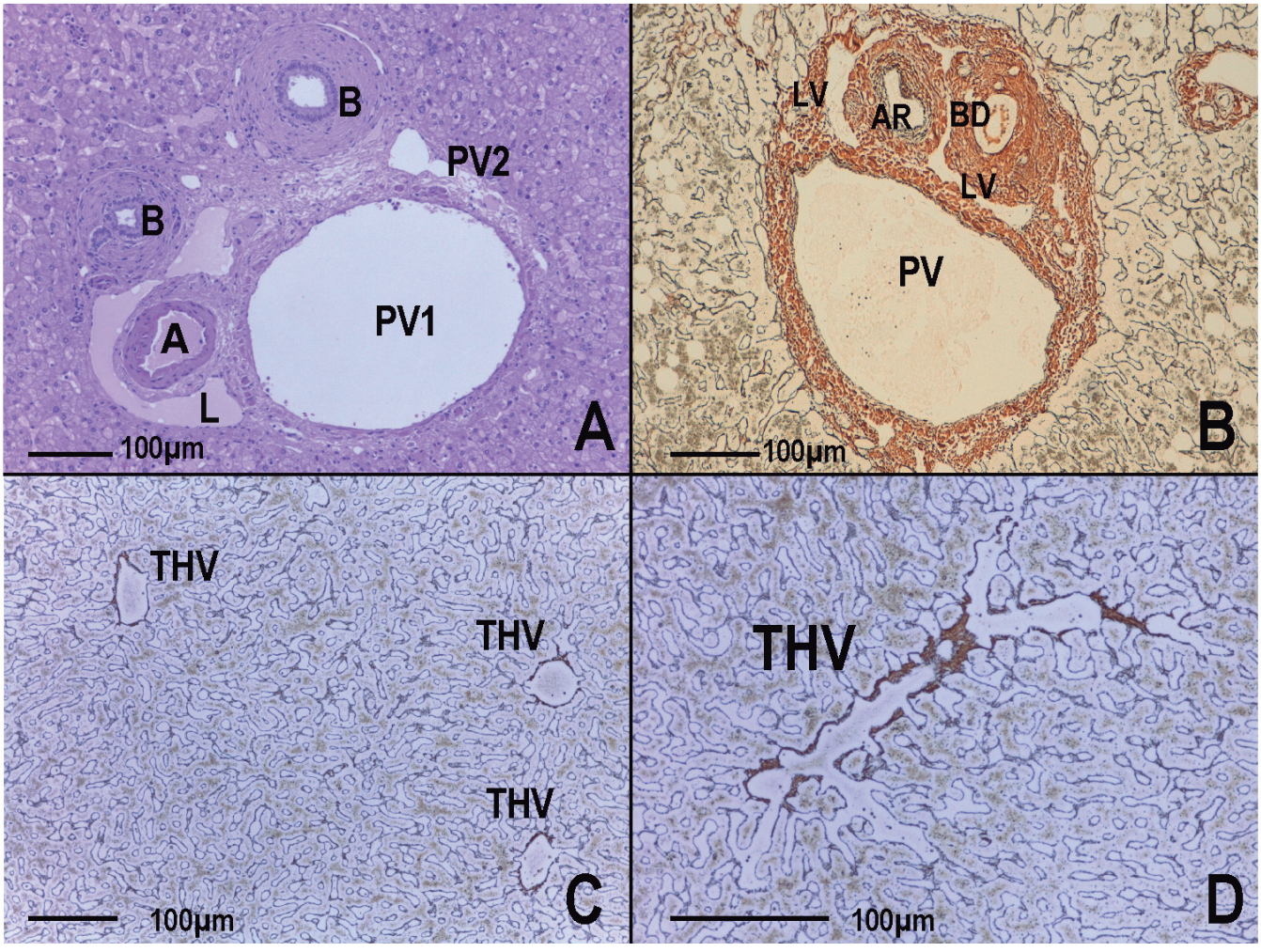

Fig. 3. A. H.E. stain. A portal tract including two PVs (case 10 in Table 2) were observed. The main PV (PV1 in the figure) with a diameter of 325 μm belongs to the vessels described by Elias (1963) in the range between 400 μm and 280 μm having mixed properties: MDVs of 50 μm (PV2 in the figure) or inlet veins can originate. PV1 is bounded by a thin muscle layer. The arteriole (A) has a well-developed wall of smooth muscle and is partially encompassed by a lymph vessel (L) "C"-shaped with pinkish material therein. The bile ducts (B) have a thick layer of smooth muscle. **B.** Reticulin stain. A lymphatic vessel (LV) of cartographic contour embracing an arteriole (AR) is observed. PV: Portal vein; BD: biliary duct. **C.** Reticulin stain. Three Terminal Hepatic Veins (THV) show a thin wall with reticulin stain. **D.** Reticulin stain. Multiple sinusoids converging in a THV. Note the thin layer of reticulin at the periphery.

have a muscular layer identifiable by conventional methods (Gibson, 1959).

To avoid sampling errors, spaces over 25 μm corresponding to lymphatic vessels, arterioles, and bile ducts, should be manually removed.

The lymph vessels in the PTs are usually collapsed virtual lumens. When distended, they contain a pinkish material (with Haemathoxylin Eosin stain) and are identified by their thin arcuate semilunar morphology bordering the hepatic arteriole (Fig. 3A,B.). Each PV is assigned an identification number with its minimum diameter. In order to avoid possible mistakes, the PTs were manually counted. We assign to each PT its corresponding vessel(s) with its diameter(s). Therefore, the distribution of veins within the PTs was analyzed and subsequently the ratio PVs/HVs was calculated according to their size.

Furthermore (Fig. 4A), it should be noted that orientation, distribution, and size of liver veins change according to their position within the liver parenchyma (Bhunchet and Wake 1998). Taking into consideration that small vessels can sprout in the hilar portion of the portal vein (Yan et al., 2014), venous distributing vessels can appear anywhere in the liver sprouting from conducting vessels of all sizes (Fig. 4B), as Kiernan already noted (1833). However, as we approach the hepatic hilum or the junction between the hepatic veins and the inferior vena cava, logically, the number of vessels per surface unit decreases. Thus, the number of meso- and microvessels per unit area changes depending on where the location of the sample was obtained. Therefore, only the ratio between the two types of venous vessels (portal and hepatic) will be statistically analyzed.

Image analysis

All the slides were examined at low magnification (4x) to select fields with better preserved morphology. For each of these fifty cases, ten photographic images per case were taken with a microscope Leica DMD108 (Leica Microsystems, Wetzlar, Germany) at 4x magnification. The surface scanned per each microphotograph was 7,655,020 μm^2. Thus, a total surface of 10x7,655,020 μm^2 was covered in each case. These ten areas were analyzed using Image-Pro Plus 7.0 software (Media Cybernetics, Silver Spring, MD, USA). The device considers only the optically empty spaces. After calibration, the system was programmed to remove spaces with a minimum diameter under 25 μm. According to Caulet et al. (1989) the inner diameter of the THVs has a value of 17.7±3.8 μm. However, if the system was programmed to delete spaces under 17.7+3.8=21.5 μm (or more), numerous sinusoids near

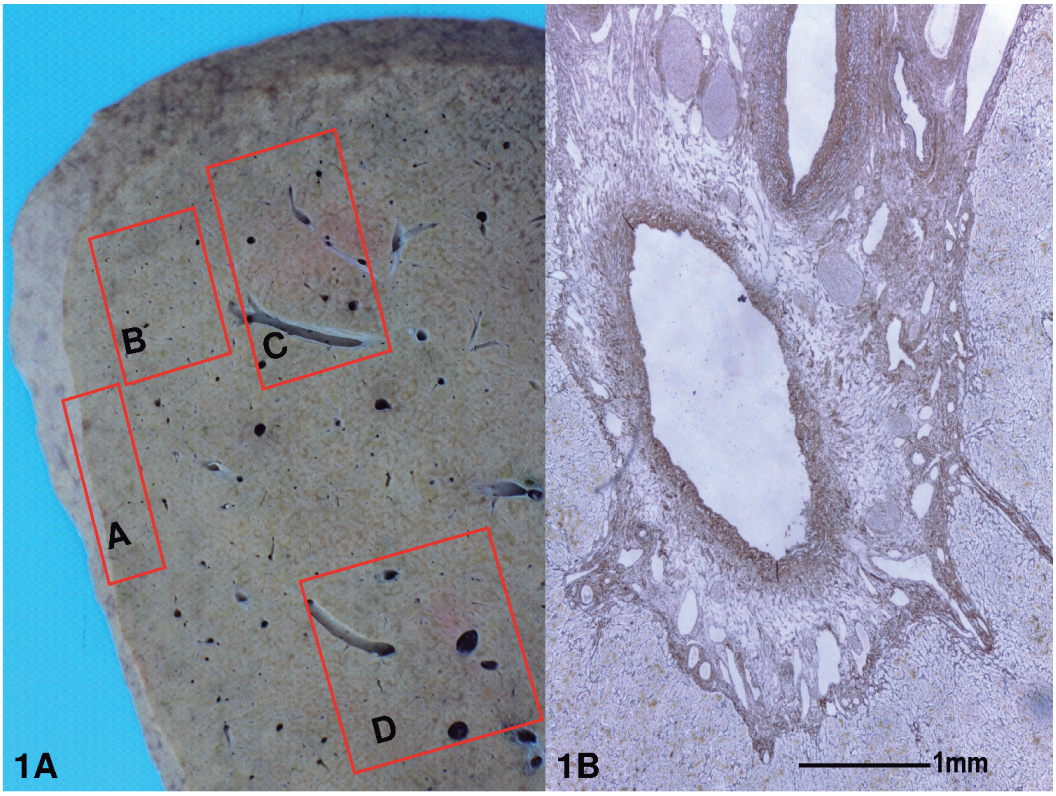

Fig. 4. A. Macro-Photography. The number of vessels per surface unit depends on the area studied. Near to Glisson capsule (rectangle A) are located the smaller vessels, however the larger are located close to the hepatic hilum (rectangle D). In areas where the vascular diameter is greater, the total number of vessels decreases. The number of vessels per surface unit according to the studied area fulfil the following inequality: A> B> C> D. **B.** Reticulin stain. Portal tracts close to the hilar region show an increased amount of connective tissue, epithelial and neural tissues with subsequent decrease in the total number of vessels per surface unit. Various distributing portal veins arise from a conducting portal vein with large-caliber.

the terminal hepatic vein would be marked. The system labels the preserved structures in red and assigns a number to each red patch (Fig. 5). Bile ducts, arteries and lymphatics were also labeled only in the larger portal tracts. Their identification numbers were manually removed, whereby only those veins whose minimum diameter was equal to or more than 25 µm were taken into consideration. Morphological analysis of the structures that surround each red stain showed whether it is a portal or hepatic venous vessel. In doubtful cases, all the slides stained with H&E and reticulin were superposed using the microanatomical criteria already established by Crawford et al. (1998) and Saxena et al. (1999).

Statistical analysis

The measurements obtained in each case will be transferred to tables that include forty intervals from 25 µm to 1000 µm (see Table 3).

We had an appropriate frequency estimation using the Chi-Square Test Statistic

$$\chi^2 = \sum_{i=1}^{n} \frac{(O_i - E_i)^2}{E_i}$$

where O_i was the observed frequency of a given variable in the i-th case, E_i is the expected frequency (given that H_0 is true) of that same variable in the i-th case and n the total number of studied cases (Daniel and Cross, 2013).

Results

Number of portal tracts and vessels in the total sample (50 cases; 3,827,510,000 µm²)

In our material, 2,996 PTs (with 3,665 PVs) and 3,761 HVs were detected (area of 50 X 76,550,200 µm²=3,827,510,000 µm²). Of the total veins, 49.3536% were PVs and 50.6463% were HVs. There were 446 PTs with more than one PV (Table 1). Of the 446 PTs, 12 PTs with a main CPV (always accompanied by more than one DPV) and 18 PTs with a main PV within the range

Table 1. The first five rows correspond to portal tracts that only contain Distributing Portal Veins (DPVs). The five last rows correspond to portal tracts that contain a Conducting Portal Vein (CPV) and several Distributing Portal Veins (DPVs).

Type of portal tract	Number of portal tracts	Number of portal veins
1 DPV	2550	2550
2 DPVs	289	578
3 DPVs	112	336
4 DPVs	25	100
5 DPVs	8	40
1 CPV+2 DPVs	4	12
1 CPV+3 DPVs	3	12
1 CPV+ 4 DPVs	3	15
1 CPV+ 7 DPVs	1	8
1 CPV + 13 DPVs	1	14
	2996	3665

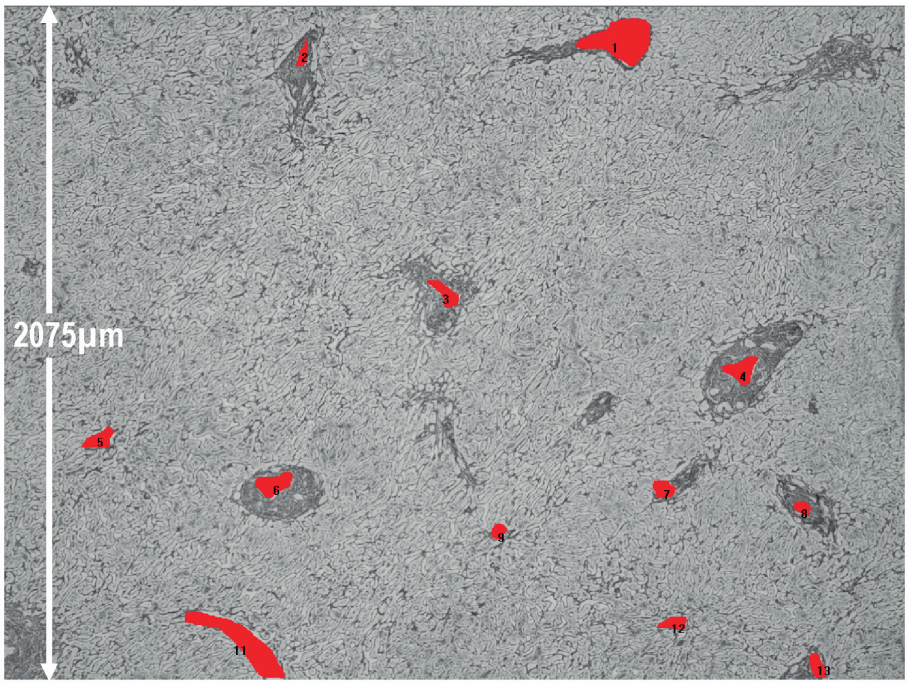

Fig. 5. Case N° 15. Reticulin stain. Image corresponding with an area of 7,655,020 µm². Each red spot is labeled with an identifying number. The morphometer establishes an univocal link between these numbers and the measured diameters. The subsequent morphological analysis can identify all the numbered spots as PVs or HVs. x 4

[280 μm , 400 μm] were noted (Table 2). In addition, 416 PTs with two or more PVs having a minimum diameter less than 280 μm were observed (Fig. 6A,B).

Size (minimum diameter) of the vessels of the total sample

Table 3 and Fig. 7 show that the interval that contains more PVs and more HVs is [30 μm, 35 μm), followed by the intervals [35 μm, 40 μm) and [40 μm, 45 μm). The minimum diameter of half of the venous vessels of both types belongs to the interval [25 μm, 60 μm), given that 1881 portal veins (49.434%) and 1924 hepatic veins (50.565%) fall within this interval.

Frequencies of PTs and HVs

According to the Kiernan model (Fig. 8A), let us consider as null hypothesis (H_0) that the PTs account for two thirds of the total population (PTs + HVs) and as H_1 hypothesis that it is different. Therefore, to test the H_0 hypothesis we assume that E_i (the expected frequency of PTs in the i-th case) is $E_i=2(O_i+\Omega_i)/3$. With the aid of Table 4 we obtain $\chi^2=520.0705$ (which is an extremely high value). The system has (2 - 1)x(50 - 1)=49 degrees of freedom. For these degrees of freedom, there is no alpha value that meets the inequality $520.0705<\alpha$. In fact, if $\alpha=0.005$, then the critical value is 78.2294 (interpolating between the tabulated values 48 and 50) and, therefore, it is not true that $520.0705<78.2294$. Analogously, if $\alpha=0.995$, then the critical value is 27.25065 and also it is not true that $520.0705<27.25065$. Logically, for the intermediate values between 0.995 and 0.005 the inequality remains unfulfilled. Therefore, the H_0 hypothesis is rejected.

If we consider Rappaport's model, the number of portal tracts is even greater (Fig. 8B). Therefore, as in the previous section, it would be impossible to defend a

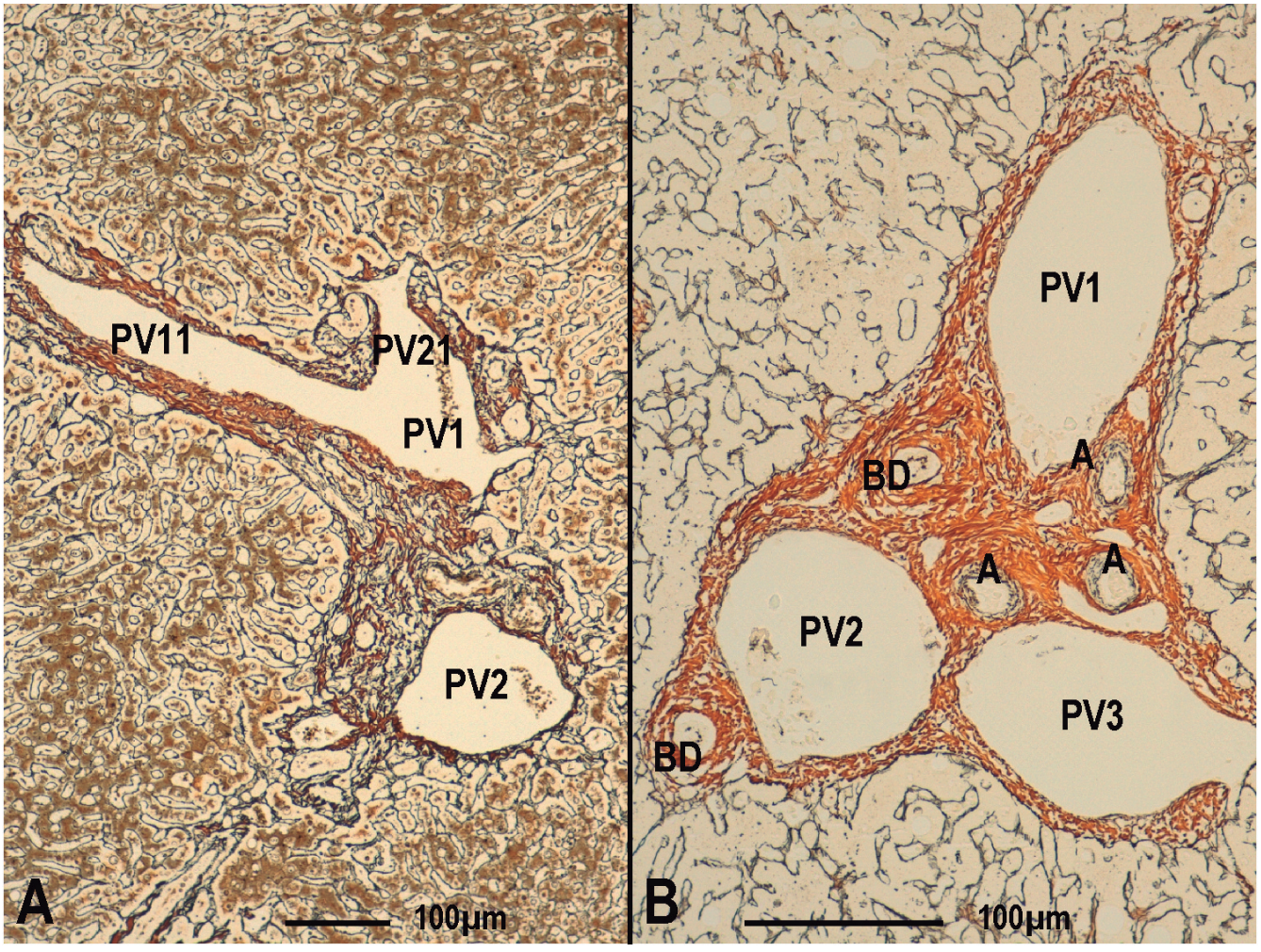

Fig. 6. A. Reticulin stain. A portal tract with two DPVs (PV1 and PV2) is observed. PV1 is divided into two new DPV (PV11 and PV21) by a branching-like process. **B.** Reticulin stain. A portal tract with three DPVs (PV1, PV2 and PV3) is observed. Three arterioles (A) and two bile ducts (BD) also appear.

similar H_0 hypothesis.

Frequencies of PVs and HVs

Let us consider as H_0 hypothesis that the total number of PVs and HVs are present with the same frequency and as H_1 hypothesis that it is different. If according to the H_0 hypothesis the number of PVs and HVs should be equal, then the expected frequency must be equal for both types of vessels. With the aid of Table 5 we obtain χ^2=27.3624. The system has (2 - 1)x(50 - 1)=49 degrees of freedom. If α=0.990, then the critical value for 49 degrees of freedom is 28.94185. Since 27.3624<28.94185, the H_0 hypothesis is not rejected.

Frequencies of PVs and HVs within the interval [25 µm, 60 µm)

Let us consider as H_0 that the PVs and HVs within the interval [25 µm, 60 µm) are present at the same frequency and as H1 that it is different. With the aid of Table 6 we obtain χ^2=14,8033. If α=0.995, then the critical value for 49 degrees of freedom is 27.25065. Since 14.8033<27.25065, the H0 hypothesis is not rejected.

Frequencies of PVs and HVs within the interval [25 µm, 400 µm)

Let us consider as H0 hypothesis that the PVs and HVs of the interval [25 µm, 400 µm) are statistically

Table 2. Characteristics of 18 portal tracts with a main portal vein whose minimum diameter lies in the range [280 µm, 400 µm].

PT	1st PV	2nd PV	3rd PV	PT	1th PV	2nd PV	3rd PV	4th PV
1	394	151	56	10	325	50		
2	393	138	56	11	322	156	62	
3	387	144	57	12	320	82	43	
4	384	365	166	13	314	98	78	
5	372	46		14	308	97	79	
6	360	45		15	302	117	49	45
7	359	76	30	16	295	114	42	
8	355	82	36	17	294	87		
9	342	121	39	18	289	130		

PT: Portal Tract. PV: Portal Vein. The minimum diameters of the companion PVs in the same tract are listed. For each PT, the vessels are sorted from highest to lowest calibres: 1st PV: First (main) Portal Vein. 2nd PV: Second Portal Vein . . . PT: Portal Tract. PV: Portal Vein.

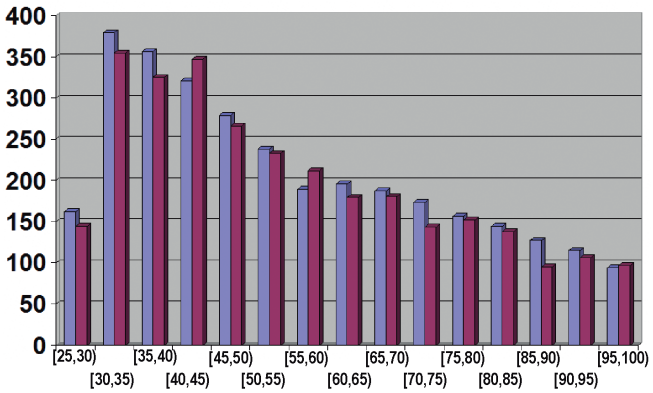

Fig. 7. Distribution of the minimum diameter of portal veins (red) and the hepatic veins (blue) along the successive 15 intervals of 5 µm length that cover the interval [25 µm ,100 µm). This numerical behaviour is as expected in a tree whose branches increase in number and decrease in diameter. The morphology and the slope of this diagram differs from those observed by Porto el al. (1989a).

Table 3. Number of portal and hepatic veins.

Interval length (µm)	Num. PVs	Num. HVs
(25,30)	144	162
(30,35)	354	379
(35,40)	325	356
(40,45)	347	321
(45,50)	266	279
(50,55)	233	238
(55,60)	212	189
(60,65)	179	195
(65,70)	180	187
(70,75)	143	173
(75,80)	152	156
(80,85)	138	144
(85,90)	95	127
(90,95)	106	115
(95,100)	97	94
(100,110)	89	98
(110,120)	106	88
(120,130)	80	77
(130,140)	88	71
(140,150)	63	52
(150,160)	41	39
(160,170)	38	35
(170,180)	19	31
(180,190)	20	22
(190,200)	22	26
(200,210)	21	25
(210,220)	23	17
(220,230)	14	12
(230,240)	16	11
(240,250)	15	9
(250,300)	12	10
(300,350)	7	4
(350,400)	8	5
(400,450)	1	2
(450,500)	1	3
(500,600)	3	2
(600,700)	2	1
(700,800)	5	3
(800,900)	0	1
(900,1000)	0	2

Num. PVs: number of portal veins belonging to each interval. Num. HVs: number of hepatic veins belonging to each interval. In this table, the first, fourth and seventh columns (in gray) contain, in ascending order, the different intervals where the minimum diameters of portal veins and hepatic veins have been included. During the first one hundred µm, the intervals have a length of 5 µm. Between 100 µm and 250 µm, the intervals are 10 µm. Between 250 µm and 500 µm, they measured 50 µm. Finally, between 500 µm and 1000 µm the length is 100 µm.

distributed in identical proportion and as H1 hypothesis that this proportion is different. With the aid of Table 7 we obtain χ^2=25.7603. If α=0.990, then the critical value for 49 degrees of freedom is 28.94185. Since 25.7603<28.94185, the H_0 hypothesis is not rejected.

Discussion

The hepatic microvasculature plays a critical role in liver histological configuration (Kiernan, 1833; Rappaport et al., 1954; Hase and Brim, 1966; Takahashi,

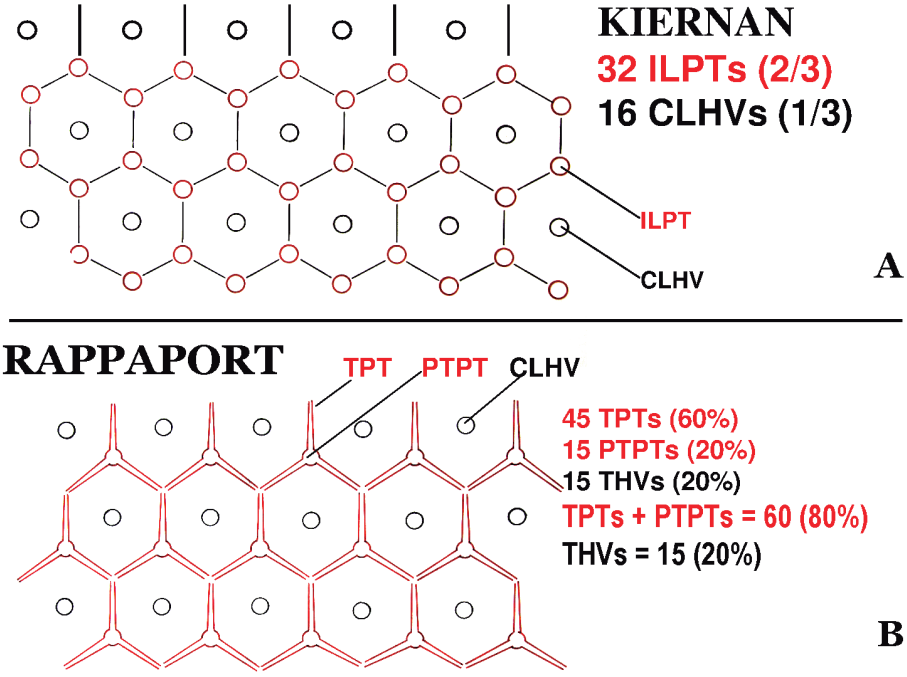

Fig. 8. Two geometric idealizations of the number and position of the portal tracts and hepatic veins of Kiernan (1833) and Rappaport (1954, 1973) models are depicted. In both descriptions, the portal tracts (regardless of their denomination and conceptual consideration) are more abundant than the hepatic veins. According to the model considered, the superabundance of portal tracts is more or less evident. ILPT: Inter-Lobular Portal Tract. CLHV: Centri-Lobular Hepatic Vein. TPT: Terminal Portal Tract. PTPT: Pre-Terminal Portal Tract.

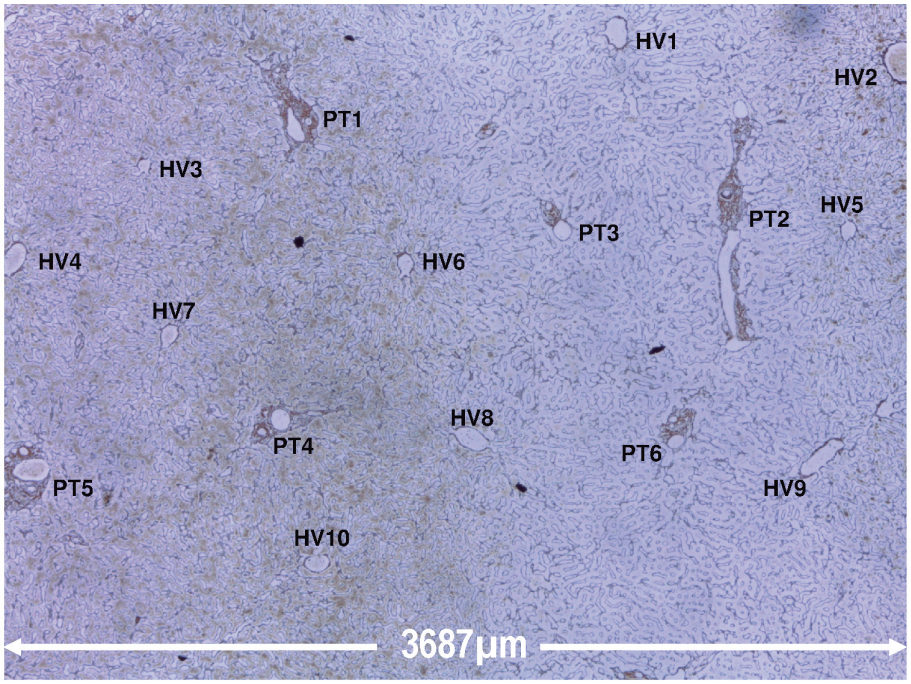

Fig. 9. 4 X Reticulin stain. The portal tracts and hepatic veins are interspersed and equally spaced. In this photomicrograph there are 6 portal tracts and 10 hepatic veins. Based upon the classic models that support the existence of subunits, the number of portal tracts should be higher than hepatic veins

1970; Rappaport, 1973; Matsumoto and Kawakami 1982; Notenboom et al., 1996; Ishikawa et al., 2000; Cast et al., 2015). The microvasculature pattern is preserved even when the liver epithelium is removed and pancreatic insular or thyroid epithelium is transplanted (Dombrowski and Evert, 2007). In addition, the hepatic vessels provide positional cues that determine the development of specific hepatocyte phenotypes (Kuo and Darnell, 1991).

In the classic models of liver there are many more PTs than HVs and, logically, there are many more PVs than HVs (Fig. 8). However, in our material (Fig. 9), fields with more HVs than PTs are easily detected. As can be seen, it is impossible to draw a polygonal line passing through five or six PTs with a single HV inside. As reported by Crawford et al. (1998) "a limited number of quantitative reports state that a percutaneous needle biopsy from an adult liver is likely to contain about 4 to

Fig. 10. Three-dimensional represen-tation of the liver structure. In the lower right quadrant, the sinusoids are interposed between the PVs (in red) and HVs (in black). Periportal domain sinusoids (in red) and pericentral domain sinusoids (in black) constitute two continuous complementary domains never intersected. The PVs as well as the HVs in this figure there are distributing veins.

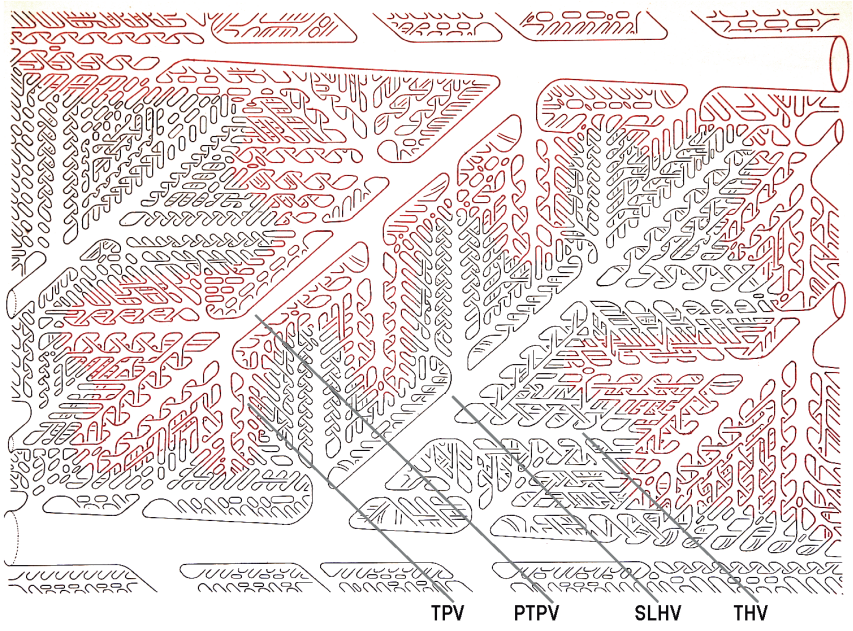

Fig. 11. Two-dimensional geometrical idealization that offers a planar version of the interdigitation principle. This schema comprises the terminal portion of a subsegmental portal vein (horizontal vessel of the upper portion in red) and the terminal portion of a collecting hepatic vein (horizontal vessel in the lower portion in black). Numerous preterminal portal veins (PTPVs) and ulterior terminal portal veins (TPVs) sprout from the former. Numerous sublobular hepatic veins (SLHVs) and ulterior terminal hepatic veins (THVs) (the classic "centrilobular vein") sprout from the latter. The vessels are arranged equidistantly, as befits Takahashi's regular interdigitation principle. Around the portal vessels we drew in red the hypothetical peri-portal domain sinusoids and around the hepatic veins the peri-hepatic-vein domain sinusoids in black. Both domains are complementary and continuous.

Table 4. Observed and expected frequencies of PTS and HVs of the 50 cases.

	PTs O_i	HVs Ω_i	PTs E_i	$\frac{(O_i - E_i)^2}{E_i}$
1	53	58	74.000	5.9594
2	45	65	73.333	10.9467
3	46	50	64.000	5.0625
4	40	62	68.000	11.5294
5	50	55	70.000	5.7142
6	66	72	92.000	7.3478
7	49	58	71.333	6.9920
8	45	68	75.333	12.2136
9	56	57	75.333	4.9615
10	53	54	71.333	4.7116
11	34	59	62.000	12.6451
12	54	55	72.666	4.7948
13	38	58	64.000	10.5625
14	78	80	105.333	7.0926
15	93	89	121.333	6.6161
16	77	82	106.000	7.9339
17	87	107	129.333	13.8563
18	75	99	116.000	14.4913
19	76	108	122.666	17.7532
20	51	74	83.333	12.5451
21	43	50	62.000	5.8225
22	54	89	95.333	17.9205
23	76	99	116.666	14.1748
24	68	96	109.333	15.6258
25	62	90	101.333	15.2673
26	50	77	84.666	14.1937
27	52	58	73.333	6.2058
28	49	64	75.333	9.2048
29	53	75	85.333	12.2510
30	75	87	108.000	10.0833
31	55	61	73.333	4.5831
32	48	67	76.666	10.7184
33	77	84	107.333	8.5723
34	35	61	64.000	13.1406
35	57	58	76.666	5.0446
36	72	64	90.666	3.8428
37	82	89	114.000	8.9824
38	76	84	106.666	8.8163
39	74	102	117.333	16.0035
40	62	91	102.000	15.6862
41	70	79	99.333	8.6620
42	66	94	106.666	15.5037
43	72	106	118.666	18.3516
44	60	79	92.666	11.5152
45	69	97	110.666	15.6873
46	75	77	101.333	6.8430
47	62	69	87.333	7.3484
48	51	79	86.666	14.6777
49	47	68	76.666	11.4792
50	38	57	63.333	10.1331

Mean of O_i: 59.92; SD of O_i: 14.508; Mean of Ω_i: 75.22; SD of Ω_i: 16.7176. PTsO_i: observed frequency of PTs of i-th case. HVsΩ_i: observed frequency of HVs of i-th case. the expected frequency of PTs of the i-th case. Note that, according to the H0 hypothesis (FIG 8A), PTs account for 2/3 of the sum of PTs + HVs. The quotient corresponds to the i-th summand of the Chi-Square Statistics. 31 of the 50 PTsO_i were included within the interval [45.412 , 74.428] (mean ± one standard deviation). On the other hand, 29 of the 50 HVsΩ_i were included within the interval [58.5024 , 91.9376] (mean ± one standard deviation).

Table 5. Observed and expected frequencies of PVs and HVs of the 50 cases.

	PTs O_i	HVs Ω_i	E_i	$\frac{(O_i - E_i)^2}{E_i}$
1	66	58	62.0	0.2580
2	52	65	58.5	0.7222
3	55	50	52.5	0.1190
4	48	62	55.0	0.8909
5	61	55	58.0	0.1551
6	80	72	76.0	0.2105
7	59	58	58.5	0.0042
8	56	68	62.0	0.5806
9	67	57	62.0	0.4032
10	65	54	59.5	0.5084
11	39	59	49.0	2.0408
12	67	55	61.0	0.5901
13	47	58	52.5	0.5761
14	95	80	87.5	0.6428
15	114	89	101.5	1.5394
16	95	82	88.5	0.4774
17	94	107	100.5	0.4203
18	92	99	95.5	0.1282
19	93	108	100.5	0.5597
20	63	74	68.5	0.4416
21	53	50	51.5	0.0436
22	66	89	77.5	1.7064
23	95	99	97.0	0.0412
24	81	96	88.5	0.6355
25	78	90	84.0	0.4285
26	60	77	68.5	1.0547
27	63	58	60.5	0.1033
28	75	64	69.5	0.4352
29	66	75	70.5	0.2872
30	92	87	89.5	0.0698
31	68	61	64.5	0.1899
32	57	67	62.0	0.4032
33	95	84	89.5	0.3379
34	43	61	52.0	1.5576
35	71	58	64.5	0.6550
36	87	64	75.5	1.7516
37	102	89	95.5	0.4424
38	93	84	88.5	0.2288
39	91	102	96.5	0.3134
40	76	91	83.5	0.6736
41	86	79	82.5	0.1484
42	81	94	87.5	0.4828
43	89	106	97.5	0.7410
44	72	79	75.5	0.1622
45	84	97	90.5	0.4668
46	90	77	83.5	0.5059
47	77	69	73.0	0.2191
48	62	79	70.5	1.0248
49	58	68	63.0	0.3968
50	46	57	51.5	0.5873

Mean of O_i: 73.3; SD of O_i: 17.5931; Mean of Ω_i: 75.22; SD of Ω_i: 16.7176. PTsO_i: observed frequency of PVs of i-th case. HVsΩ_i: observed frequency of HVs of i-th case. the (same) expected frequency for both PVs and HVs of the i-th case. Note that, according to the H0 hypothesis, the expected frequency is equal for both types of veins. The quotient corresponds to the i-th summand of the Chi-Square Statistics. 30 of the 50 PTsO_i were included within the interval [55.7069 , 90.8931] (mean ± one standard deviation). Logically, the mean and the standard deviation of the 50 HVsΩ_i were the same as in the previous section (Table 4).

6 portal tracts, matched by an approximately equal number of terminal hepatic veins". Consequently, it seems reasonable to calculate the ratio of these structures in large liver tissue samples instead in Tru-Cut liver biopsies.

In the present study, 2,996 portal tract (triads) and 3,761 hepatic veins were counted. This quotient (2,996/3,761) is justified by the fact that there was more

Table 6. Observed and expected frequencies of PVs and HVs within the interval [25 µm, 60 µm).

	PTs (25,60) O_i	HVs (25,60) Ω_i	E_i	$\frac{(O_i - E_i)^2}{E_i}$
1	34	29	31.5	0.1984
2	31	37	34.0	0.2647
3	32	26	29.0	0.3103
4	29	34	31.5	0.1984
5	30	34	32.0	0.1250
6	37	36	36.5	0.0068
7	33	29	31.0	0.1290
8	39	30	34.5	0.5869
9	33	35	34.0	0.0294
10	29	31	30.0	0.0333
11	19	27	23.0	0.6956
12	32	28	30.0	0.1333
13	26	31	28.5	0.2192
14	47	39	43.0	0.3720
15	55	42	48.5	0.8711
16	37	40	38.5	0.0584
17	40	52	46.0	0.6956
18	38	46	42.0	0.3809
19	49	53	51.0	0.0784
20	39	45	42.0	0.2142
21	27	22	24.5	0.2604
22	42	33	37.5	0.5400
23	37	43	40.0	0.2250
24	42	50	46.0	0.3478
25	38	47	42.5	0.4764
28	32	39	35.5	0.3450
27	33	24	28.5	0.7105
28	37	32	34.5	0.1811
29	34	39	36.5	0.1712
30	53	58	55.5	0.1126
31	36	33	34.5	0.0652
32	29	25	27.0	0.1481
33	42	36	39.0	0.2307
34	26	29	27.5	0.0818
35	37	32	34-5	0.1811
36	46	37	41.5	0.4879
37	53	46	49.5	0.2474
38	47	42	44.5	0.1404
39	68	60	64.0	0.2500
40	59	66	62.5	0.1960
41	36	42	39.0	0.2307
42	37	40	38.5	0.0584
43	42	51	46.5	0.4354
44	46	59	52.5	0.8047
45	35	42	38.5	0.3181
46	38	35	36.5	0.0616
47	34	28	31.0	0.2903
48	27	32	29.5	0.2118
49	36	45	40.5	0.5000
50	23	33	28.0	0.8928

Mean of O_i: 37.62; SD of O_i: 9.35; Mean of Ω_i: 34.48; SD of Ω_i: 10.0736. The symbols have the same formal meaning as the previous figure. 35 of the 50 PTsO_i were within the interval [28.27 , 46.97] (mean ± one standard deviation). On the other hand, 35 cases of the 50 HVsΩ_i were within the interval [28.4064 , 48.5536] (mean ± one standard deviation).

Table 7. Observed and expected frequencies of PVs and HVs within the interval [25 µm, 400 µm).

	PTs (25,400) O_i	HVs (25,400) Ω_i	E_i	$\frac{(O_i - E_i)^2}{E_i}$
1	66	58	62.0	0.2580
2	52	65	58.5	0.7222
3	55	50	52.5	0.1190
4	48	61	54.5	0.7752
5	61	55	58.0	0.1551
6	78	72	75.0	0.1200
7	59	58	58.5	0.0042
8	56	68	62.0	0.5806
9	67	57	62.0	0.4032
10	65	54	59.5	0.5084
11	39	59	49.0	2.0408
12	67	55	61.0	0.5901
13	47	58	52.5	0.5761
14	94	79	86.5	0.6502
15	112	89	100.5	1.3159
16	95	82	88.5	0.4774
17	93	106	99.5	0.4246
18	92	98	95.0	0.0947
19	93	107	100.0	0.4900
20	63	74	68.5	0.4416
21	53	50	51.5	0.0436
22	66	88	77.0	1.5714
23	91	99	95.0	0.1684
24	85	95	90.0	0.2777
25	78	89	83.5	0.3622
26	60	77	68.5	1.0547
27	63	58	60.5	0.1033
28	75	64	69.5	0.4352
29	66	75	70.5	0.2872
30	91	86	88.5	0.0706
31	68	61	64.5	0.1899
32	57	67	62.0	0.4032
33	94	84	89.0	0.2808
34	43	61	52.0	1.5576
35	71	58	64.5	0.6550
36	86	64	75.0	1.6133
37	99	88	93.5	0.3235
38	93	84	88.5	0.2288
39	91	102	96.5	0.3134
40	76	91	83.5	0.6736
41	86	79	82.5	0.1484
42	81	94	87.5	0.4828
43	89	104	96.5	0.5829
44	72	79	75.5	0.1622
45	84	96	90.0	0.4000
46	90	77	83.5	0.5059
47	77	69	73.0	0.2191
48	62	78	70.0	0.9142
49	58	68	63.0	0.3968
50	46	57	51.5	0.5873

Mean of O_i: 73.06; SD of O_i: 17.2323; Mean of Ω_i: 79.94; SD of Ω_i: 16.4272. 30 of the 50 PTsO_i were included within the interval [55.8277 , 90.2923] (mean ± one standard deviation). 29 of the 50 HVsΩ_i were included within the interval [58.5128 , 91.3672] (mean ± one standard deviation).

than one PV in 446 PTs. In contrast, in the study reported by Crawford et al. (1998) using needle biopsies, the ratio PTs/HVs is 175/115. The discordant results could be explained by significant differences in sample size and the histological characteristics of the material.

Out of 446 PTs with more than one PV, 12 contained a CPV (always accompanied by more than one DPV) and 18 PTs with a main PV whose minimum diameter lies in the range [280 μm, 400 μm]. Moreover, 416 PTs showed two or more PVs having a minimum diameter less than 280 μm. These results are inconsistent with the definition of ADV by Elias (1963) considering that ADVs have a diameter less than 280 μm and these structures are not accompanied by another portal vessel.

In fact, few studies provide histomorphometric data on the size and distribution of the portal and hepatic veins. Porto et al. (1989a) performed a histomorphometric study on the THVs (those with internal diameter ≤150 μm, according to the quantitative criteria of these authors) on a surface of 112 mm^2 (14 frames of 8 mm^2) of both humans and baboons. On this surface, 93 THVs were observed in human samples (74% of all hepatic veins) and 99 THVs in baboons (84% of all hepatic veins). In their study (Porto et al. 1989a) the number of THVs between 30 to 70 μm was basically constant, decreasing slowly between 70 to 100 μm and drastically decreasing above 100 μm.

The morphometric studies of the hepatic vascular tree focused predominantly on aspects related to pathologic processes (Wanless, 1987; Imamura et al., 1994; Porto el al., 1989b). Moreover, there are many studies of vascular corrosion casts (Del Rio Lozano and Andrews, 1966; McCuskey et al., 2003; Andrews and Andrews, 1976; Debbaut et al., 2014).

In our material, the largest contingent of vessels belong predominantly to the micro- and meso-circulation in the sense defined by Debbaut et al. (2014). First generations of PVs and HVs were less frequent, considering that liver samples from autopsy were obtained predominantly from the subcapsular territory in order to exclude a hypothetical parenchymal disease. It is important to remark that in the present study we detected 3,449 HVs within the interval [25 μm, 150 μm) that suppose 92.690% of all HVs. Indeed, in the study published by Porto et al. (1989a), these veins constitute 74% of all HVs in humans and 84% in baboons. However, the surface measured by these authors was lower compared with the present study.

Analyzing the schemata of Kiernan (1833), Rappaport et al. (1954) and Rappaport (1973) reveals a preponderance of PTs over the HVs (regardless of their denomination and conceptual consideration). According to the Kiernan model there must be double the number of ILPTs than CLHVs (Fig. 8A). Moreover, in the Rappaport model, the distribution should be 80% PTs (of these, 20% are PTPTs and 60% TPTs) and 20% THVs (CLHVs) (Fig. 8B). However, The difference between the observed and the expected frequencies is so high that this hypothesis is rejected for all values of alpha.

The presence of an equivalent number (from a statistical point of view) of both types of distributing veins is compatible with the principle of interdigitation (Takahashi, 1970). Figures 10 and 11 represent the structural schema of the hepatic vasculature. The regular and equidistant vascular interdigitation implies the existence of the same number of vessels of both venous systems. Moreover, it is compatible with the presence of a continuous empty space which may be occupied by a continuous mass of liver parenchyma. This parenchymatous mass consists of two domains: periportal and pericentral (around the HVs).

Finally, we accept that the presence of an equivalent number of functional (nonconducting) hepatic and portal veins does not provide sufficient data to develop a histological liver model. Nevertheless, the present findings open a new window for new models of liver microcirculatory system. The numerical equivalence of the functional vessels of both systems is incompatible with the models of Kiernan (1833), Matsumoto and Kawakami (1982) and Rappaport et al. (1954). Moreover, the model proposed by Elias (1949a; 1949b) provides a satisfactory qualitative explanation of hepatic architecture, but does not study the number distribution and spatial relationships of the hepatic and portal veins. We consider that the present results are compatible with the vascular model proposed by Takahashi (1970).

Therefore, we support the hypothesis that, in the distal portions, the branching scheme produces portal vessels alternatively intermingled with corresponding branches of the hepatic veins.

Acknowledgements. Our sincere thanks to Drs. Isidro Machado and Francisco Gozalbo for their invaluable assistance in selecting appropriate samples.

References

Andrews C.J. and Andrews W.H. (1976). Casts of hepatic blood vessels: A comparison of the microcirculation of the penguin, Pygoscelis adelia, with some comon laboratory animals. J. Anat. 122, 283-292.

Bhunchet E. and Wake K. (1998). The portal lobule in rat liver fibrosis: a re-evaluation of the liver unit. Hepatology 27, 481-487.

Cast A.E., Walter T.J. and Huppert S.S. (2015). Vascular patterning sets the stage for macro and microhepatic architecture. Dev. Dyn. 244, 498-506.

Caulet S., Fabret M., Schoevaert D., Lesty C., Meduri G. and Martin E. (1989). Quantitative study of centrilobular hepatic fibrosis in alcoholic disease before cirrhosis. Virch. Arch. A 416, 11-17.

Crawford A.R., Lin X.Z. and Crawford J.M. (1998). The normal adult human liver biopsy: A quantitative reference standard. Hepatology 28, 323-331.

Daniel W.W. and Cross C.L. (2013). Biostatistics: A foundation for analysis in the health sciences. 10th Edition. John Wiley & Sons, Inc., Hoboken, NJ. pp 600-669.

Debbaut C., Segers P., Cornillie P., Casteleyn C., Dierick M., Lateman W. and Monbaliu D. (2014). Analyzing the human liver vascular

architecture by combining vascular corrosion casting and micro-CT scanning: a feasible study. J. Anat. 224, 509-517.

Del Rio Lozano I. and Andrews W.H. (1966). A study by means of vascular casts of small vessels related to the mammalian portal vein. J. Anat. 100, 665-673.

Dombrowski F. and Evert M. (2007). Revelation of simple and complex liver acini after portal transplantation of pancreatic islets or thyroid follicles in rats. Hepatology 45, 705-715

Ekataksin W. (2000). The isolated artery: An intrahepatic arterial pathway that can bypass the lobular parenchyma in mammalian livers. Hepatology 31, 269-279.

Elias H. (1949a). A re-examination of the structure of the mammalian liver. I. Parenchymal architecture. Am. J. Anat. 84, 311-333.

Elias H. (1949b). A re-examination of the structure of the mammalian liver. II. The hepatic lobule and its relation to the vascular and biliary sytems. Am. J. Anat. 85, 379-456.

Elias H. (1963). Anatomy of the liver. In: The liver: Morphology, biochemistry, physiology. Rouiller C. (ed). Academic Press. New York. pp 41-59.

Gibson J.B. (1959). The hepatic veins in man and their sphincter mechanisms. J. Anat. 93, 368-379.

Hase T. and Brim J. (1966). Observation on the microcirculatory architecture of the rat liver. Anat. Rec. 156, 157-173.

Imamura H., Kawasaki S., Bandai Y., Sanjo K. and Idezuki Y. (1994). Morphometry of sinusoids and portal hypertension in non-alcoholic cirrhosis. J. Hepatol. 21, 167-173.

Ishikawa T., Mori M., Ichikawa Y., Kitoh J. and Yamashita K. (2000). Three-dimensional observations of spatial arrangement of hepatic zonation and vein system in mice and house musk shrews. Anat. Rec. 260, 228-237.

Jones A.L. and Spring-Mills E. (1982). Hígado y vesícula biliar. In: Histología. 4th ed. Weiss L. and Greep R.O. (eds). El Ateneo. pp 624-664.

Kiernan F. (1833). The anatomy and physiology of the liver. Philos. Trans. R. Soc. Lond. 123, 711-770.

Korzh S., Pan X., García-Lecea M., Winata C.L., Pan X., Wohland T., Korzh W. and Gong Z. (2008). Requirement of vasculogenesis and blood circulation in late stages of liver growth bin zebrafish. BMC Dev. Biol. 8:84.

Kuo F.C. and Darnell J.E. (1991). Evidence that interaction of hepatocytes with the collecting (hepatic) veins triggers position-specific transcription of the glutamine synthetase and ornithine aminotransferase genes in the mouse liver. Mol. Cell. Biol. 11, 6050-6058.

Lamers W.H., Hilberts A., Furt E., Smith J., Jonges G.N., van Noorden C.J., Janzen J.W., Charles R. and Moorman A.F. (1989). Hepatic enzymic zonation: a reevaluation of the concept of the liver acinus. Hepatology 10, 72-76

Mall F. (1906). A study of the structural unit of the liver. Am. J. Anat. 5, 227-308.

Matsumoto T. and Kawakami M. (1982). The unit-concept of hepatic parenchyma: a re-examination based on angioarchitectural studies. Acta Pathol. Jpn. 32 (Suppl 2), 285-314.

Matsumoto K., Yoshitomi H., Rossant J. and Zaret K.S. (2001). Liver organogenesis promoted by endothelial cells prior to vascular function. Science 294, 559-563.

Matsumoto K., Miki R., Nakayama M., Tatsumi N. and Yokouchi Y. (2008). Wnt9a secreted from the walls of hepatic sinusoids is essential for morphogenesis, proliferation, and glycogen accumulation of chick hepatic epithelium. Dev. Biol. 319, 234-247.

McCuskey R.S. (2008). The hepatic microvascular system in health and its response to toxicants. Anat. Rec. 291, 661-671

McCuskey R.S. (1993). Functional morphology of the liver with emphasis on its microvasculature. In: Hepatic anion transport and bile secretion: physiology and patho-physiology. Tavoloni N. and Berk P. (eds). Raven Press. New York. pp 1-10.

McCuskey R.S. (1994). The hepatic microvascular system. In: The liver: biology and pathobiology. 3rd ed. Arias I.M., Boyer J.L., Fausto N., Jakoby W.B., Schachter D. and Shafritz D.A. (eds). Raven Press. New York. pp 1089-1106.

McCuskey R.S., Ekataksin W., LeBouton A.V., Nishida J., McCuskey M.K., McDonnell D., Williams C., Bethea N.W., Dvorak B. and Koldovsky O. (2003). Hepatic microvascular development in relation to the morphogenesis of hepatocellular plates in neonatal rats. Anat. Rec. Part A. 275, 1019-1030.

Nakamura Y. and Takahashi T. (1998). A computer-aided 3-D geometry of acute and chronic zonal necrosis: Three-D tangent counting applied in an attempt to re-examine the structure of the human liver. Tohoku. J. Exp. Med. 184, 207-227.

Notenboom R.G.E., de Boer P.A.J., Moorman A.F.M. and Lamers W.H. (1996). The establishment of the hepatic architecture is a prerequisite for the development of a lobular pattern of gene expression. Development 122, 321-332.

Porto L.C., Chevallier M. and Grimaud J.A. (1989a). Morphometry of terminal hepatic veins. 1. Follow up in chronically alcohol-fed baboons. Virchows Arch. A 414, 129-134.

Porto L.C., Chevallier M. and Grimaud J.A. (1989b). Morphometry of terminal hepatic veins. 2. Comparative study in man and baboon. Virchows Arch. A 414, 299-307.

Rappaport A.M. (1973). The microvascular hepatic unit. Microvasc. Res. 6, 212-228.

Rappaport A.M., Borowy Z.J., Lougheed W.M. and Lotto W.N. (1954). Subdivision of hexagonal liver lobules into a structural and functional unit: Role in hepatic physiology and pathology. Anat. Rec. 119, 11-33.

Rømert P., Quistorff B. and Bhenke O. (1993). Histological evaluation of the zonation of colloidal gold uptake by the rat liver. Tissue Cell 25, 19-32

Saxena R., Theise N.D. and Crawford J.M. (1999). Microanatomy of the human liver - exploring the hidden interfaces. Hepatology 30, 1339-1346.

Takahashi T. (1970). Lobular structure of the human liver from the viewpoint of hepatic vascular architecture. Tohoku J. Exp. Med. 101, 119-140.

Wanless I.R. (1987). The use of morphometry in the study of nodular and vascular lesions of the liver. Anal. Quant. Cytol. Histol. 9, 39-41.

Wanless I.R., Nakashima E, and Sherman M. (2000). Regression of human cirrhosis. Morphological features and genesis of incomplete septal cirrhosis. Arch. Pathol. Lab. Med. 124, 1599-1607.

Yan P-N., Tan W-F., Yang X-W., Zhang C-S. and Jiang X-Q. (2014). Applied anatomy of small branches of the portal vein in transverse groove of hepatic hilum. Surg. Radiol. Anat. 36, 1071-1077.

Accepted September 23, 2016